Magnetization and neutron-diffraction studies of magnetic properties of single-crystal $DyMn_2Ge_2$

Hisao Kobayashi
Electrotechnical Laboratory, 1-1-4 Umezono, Tsukuba, Ibaraki 305, Japan

Hideya Onodera, Yasuo Yamaguchi, and Hisao Yamamoto
Institute for Materials Research, Tohoku University, 2-1-1 Katahira, Sendai, Miyagi 980, Japan
(Received 1 December 1989; revised manuscript received 19 September 1990)

Magnetic properties of single-crystal $DyMn_2Ge_2$ have been studied by magnetization measurement in high fields up to 150 kOe and by neutron diffraction. Four magnetically ordered phases have been observed. In low magnetic fields parallel to the [001] direction, collinear antiferromagnetism is observed in the temperature range from 37.5 to 431 K with the Mn moments ferromagnetically coupled on the (001) layers, and with antiferromagnetic coupling between the adjacent (001) Mn layers. Below 33 K, there is a collinear ferrimagnetic structure with the Dy and Mn moments antiparallel to each other along the c axis. A new magnetic phase is observed in the temperature range between 33 and 37.5 K, where its magnetic structure is not uniquely determined but the averaged moments at the Dy and the Mn atoms are evaluated to be about $6\mu_B$ and $1\mu_B$, respectively. Another new magnetic phase is observed in high magnetic fields along the [001] directions below 65 K. The magnetic structure of this phase, which has been deduced from the magnetization measurement, is a canted ferrimagnetic structure, with the Dy moments oriented along the c axis, and the Mn moments canted away from the c axis.

I. INTRODUCTION

In recent years many experimental studies have been reported on intermetallic compounds of the composition RM_2X_2 (R = a rare earth or Y, M = a transition metal, and X = Si or Ge) because these intermetallic compounds display a variety of interesting magnetic properties and other related effects, e.g., heavy-fermion superconductivity, valence fluctuations, or the Kondo effect. The RM_2X_2 compounds crystallize in a simple body-centered tetragonal $ThCr_2Si_2$-type structure with space group $I4/mmm$ (D_{4h}^{17}), in which the R, M, and X atoms occupy the 2(a), 4(d), and 4(c) crystallographic sites, respectively. This structure may be described as a stacking of atomic layers along the c axis with a $-M-X-R-X-M-$ sequence. The spacings between adjacent (001) R layers and adjacent (001) M layers are both $c/2$ (~ 5 Å), and are much larger than the nearest R-R and the M-M distances within the (001) layers ($a \sim 4$ Å) and $a/\sqrt{2} \sim 2.8$ Å, respectively).

It has been shown that the M atoms carry no magnetic moment[1] in most of the RM_2X_2 compounds (except for M = Mn). In contrast, in RMn_2Ge_2 systems, the Mn sublattice becomes magnetically ordered at relatively high temperatures.[2,3] Studies of these systems have been focused on the Mn-Mn as well as the R-Mn interactions. From magnetization measurements, it has been found that in the Gd, Tb, Dy, Ho, and Er compounds, Mn moments are ordered antiferromagnetically, and the magnetization sharply increases with decreasing temperature.[2,3] In particular, magnetization measurements carried out on $GdMn_2Ge_2$ single crystals have shown that the antiferromagnetic ordering of Mn moments occurs at $T_N = 365$ K, and that there is another transition to a ferrimagnetic state at 96.5 K.[4,5] These experimental results suggest that the magnetic structure of the Mn sublattice changes from antiferromagnetic to ferromagnetic. In addition to that result, two new magnetic phases have been observed in high magnetic fields,[5] showing that the Gd-Mn and Mn-Mn exchange interactions in this compound compete with each other.

Usually, in rare-earth (R)-3d-transition-metal (3d) compounds, where the R and 3d atoms have magnetic moments, the 3d-R exchange interaction is weaker than that of 3d-3d, but decidedly stronger than the R-R exchange interaction. Except for the Gd compounds, the magnetic anisotropy of these materials is dominated by the crystalline electric fields acting on the R ions. For instance, in contrast with $GdMn_2Ge_2$, $DyMn_2Ge_2$ has a large magnetic anisotropy due to the electronic configuration of the Dy^{3+} ion ($^6H_{15/2}$) and the uniaxial symmetry of the 2(a) site ($4/mmm$). From the magnetization measurements of $DyMn_2Ge_2$, moreover, it is suggested that the Dy-Mn and the Mn-Mn exchange interactions compete with each other.[2,3] Therefore, this compound is expected to develop interesting magnetic properties because a magnetic structure stabilized by competing interaction can easily be modified by an external field and/or temperature change.

In the present study, we have investigated the magnetic properties of single-crystal $DyMn_2Ge_2$ in high magnetic fields up to 150 kOe and have found the first reliable evidence for the existence of two new magnetic phases. In addition to the above results, we report a model for the magnetic structure of each phase of $DyMn_2Ge_2$ on the basis of neutron-diffraction experiments.

II. EXPERIMENT

Appropriate amounts of the starting materials Dy (99.9% purity), Mn (99.9% purity), and Ge (99.999% purity) were melted into a polycrystalline ingot by standard argon arc methods. The formation of the single-phase compound was checked by x-ray diffraction. The single crystal used in this study was grown by the Bridgman method, followed by annealing at 850 °C for about 50 h.

The magnetization was measured as a function of temperature and magnetic field using a vibrating sample magnetometer. The temperature dependence of the magnetization was measured in the range from 4.2 to 650 K. High magnetic fields (up to 150 kOe) were produced using a Bitter-type magnet at the High Field Laboratory for Superconducting Materials at Tohoku University. The mass of single-crystal $DyMn_2Ge_2$ used in this magnetization measurement was about 15 mg.

Neutron diffraction was carried out at the KID diffractometer installed at the JRR-2 reactor in JAERI using an incident neutron beam with $\lambda = 1.006$ Å from a (002) pyrolytic-graphite monochromater. The single-crystal $DyMn_2Ge_2$ was cut into a $0.7 \times 3.0 \times 0.95$ mm^3 parallelepiped with its long edge parallel to the [010] axis. The sample was mounted with the [010] axis vertical so that the $(h0l)$ reflections could be observed. This experimental geometry diminished the effects of the large neutron-absorption cross section of natural dysprosium (535 b at 1.08 Å). The integrated intensities of various reflections were measured at 8, 35, and 50 K. Detailed studies of the temperature dependence of the integrated intensities were carried out for the (101) and (201) reflections.

III. RESULTS AND ANALYSIS

A. Magnetization measurements

The temperature dependence of the magnetization $M(T)$ was measured along three directions at 10 kOe in a range from 4.2 to 650 K. A small but clear cusp corresponding to a Néel transition was observed at 431 K. Figure 1 shows the $M(T)$ characteristics obtained for these three directions in the temperature range below 77 K. The ⟨001⟩ magnetization data displayed in this figure exhibit two distinct steplike features at $T_1 = 33$ K and $T_2 = 42$ K, clearly indicating two magnetic phase transitions. Usually, when the $M(T)$ characteristic shows a sharp discontinuity at some magnetic field, the transition temperature is sensitive to the applied magnetic field. In order to determine the transition temperature in the $H = 0$ limit, the temperature dependence of the magnetization along the ⟨001⟩ direction was measured in various magnetic fields in a range from 4.2 to 77 K. Since the value of T_1 was found not to depend significantly on the magnetic field below 10 kOe, we could easily obtain the transition temperature as $T_{c1} = 33.0 \pm 0.5$ K by extrapolating T_1 to $H = 0$. In contrast, the value of T_2 appeared to be quite sensitive to the applied magnetic field and increased with increasing magnetic field up to 15 kOe. By extrapolating the T_2 data

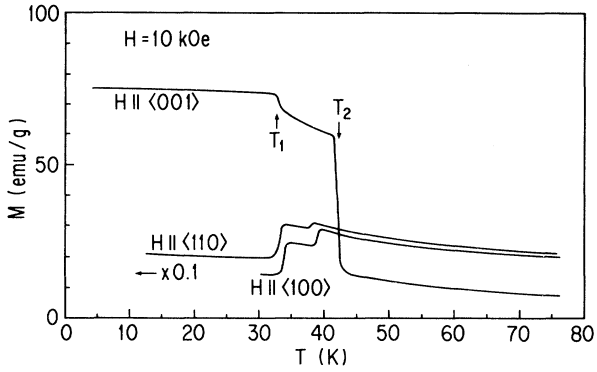

FIG. 1. Temperature dependence of magnetization along the three directions at 10 kOe. T_1 and T_2 indicate the magnetic transition temperatures. The Néel temperature T_N is 431 K.

linearly to $H = 0$, we obtained the transition temperature as $T_{c2} = 37.5 \pm 0.5$ K. These transition temperatures are consistent with the temperatures where the magnetizations along the ⟨100⟩ and ⟨110⟩ directions change discontinuously.

Figure 2 shows the magnetization $\sigma(H)$ measured for the three directions at various temperatures in applied fields up to 150 kOe. The data displayed in Fig. 2(a) (for 4.2 K $< T_{c1}$) clearly indicate that the easy direction of magnetization is the c axis, and that the anisotropy within the c plane is very small. A sharp jump is clearly seen in the $\sigma(H)$ curve for the ⟨001⟩ direction around the critical field $H_{c1} = 70$ kOe, and the increment of $\sigma(H)$ is about $2\mu_B$/formula-unit (f.u.). The spontaneous magnetization (σ_s) below H_{c1} is found to be $5.6\mu_B$/f.u. (after correcting for the demagnetizing fields), which is much smaller than the theoretical value ($10\mu_B$) of the Dy^{3+} free ion with the electronic configuration of $^6H_{15/2}$. Such a disagreement between these two values suggests that the Mn atom also carries a magnetic moment, and these Mn moments couple antiferromagnetically with the Dy moments. Assuming that the Dy atom actually has the moment of $10\mu_B$, and that the Dy and Mn moments are antiparallel to each other and oriented along the c axis, the magnitude of the Mn moment can be estimated to be $2.2\mu_B$. In contrast to the behavior observed for the ⟨001⟩ direction, the $\sigma(H)$ curve in the c plane shows only a linear increase with the magnetic field up to H as high as 120 kOe. As shown in Fig. 2(b) (for 20 $K < T_{c1}$), both σ_s and the increment of $\sigma(H)$ at H_{c1} take the same values as those at 4.2 K. Hence it is considered that these values are independent of temperature between 4.2 K and T_{c1}, but the value of H_{c1} gradually decreases with increasing temperature.

As clearly seen in Fig. 2(c) (for $T_{c1} < 35$ K $< T_{c2}$), the $\sigma(H)$ curve for the ⟨001⟩ direction at 35 K differs significantly from those below T_{c1}. The value of σ_s is found to be $4.5\mu_B$/f.u. (after correcting for demagnetizing fields). The magnetization increases almost linearly with applied magnetic field up to 50 kOe and deviates from this linear increase line around the critical field

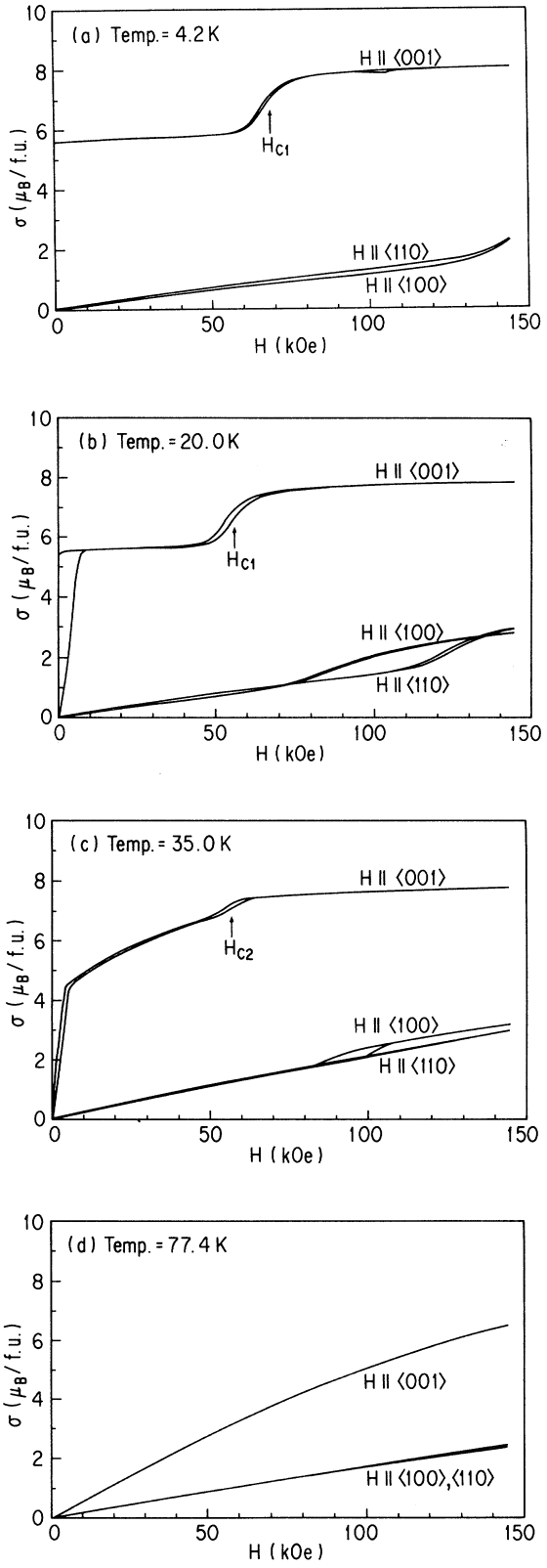

FIG. 2. Magnetization per formula unit (f.u.) as a function of applied magnetic field along the three directions. Two magnetic transition temperatures T_{c1} and T_{c2} are 33.0 and 37.5 K, respectively. (a) 4.2 K, (b) 20 K, (c) 35 K, and (d) 77.4 K.

$H_{c2}=60$ kOe. The value of $\sigma(H)$ above 70 kOe coincides with that above H_{c1} and below T_{c1}. The value of H_{c2} is quite sensitive to temperature and increases with increasing temperature. The anisotropy within the c plane is very small.

As shown in Fig. 2(d) (for 77.4 K $> T_{c2}$), the value of σ_s disappears above T_{c2}. The susceptibility along the c axis is larger than that in the c plane, and this anisotropic behavior differs from that of $GdMn_2Ge_2$.[5] In the temperature range from T_{c2} to about 60 K, the $\sigma(H)$ curve along the ⟨001⟩ direction shows a sharp jump at the critical field H_{c3}, and this curve is almost linear above H_{c3} up to H_{c2}, and finally deviates from this linear increase line around H_{c2}. This $\sigma(H)$ behavior above H_{c3} is similar to that in the range from T_{c1} to T_{c2}. The value of H_{c3} increases rapidly, while the increment of $\sigma(H)$ at H_{c3} decreases with increasing temperature.

The critical fields are determined from the magnetization measurement and shown in Fig. 3 as a function of temperature. It is found that there are four magnetically ordered phases. As observed in $GdMn_2Ge_2$ (Refs. 4 and 5) and $TbMn_2Ge_2$,[4] the magnetic structures of phases I and II seem to be ferrimagnetic and antiferromagnetic, respectively.

B. Neutron-diffraction experiments

All of the reflections observed at 8, 35, and 50 K can be indexed on the basis of the tetragonal unit cell. The nuclear and magnetic data were fitted to the calculated intensities by the least-squares method. In this procedure, two corrections were taken into account.

(1) The secondary extinction effect was corrected using the relation[6]

$$I_{\text{obs}}=aI_{\text{calc}}/\sqrt{1+bI_{\text{calc}}}\ ,$$

where I_{obs} and I_{calc} are, respectively, the observed and

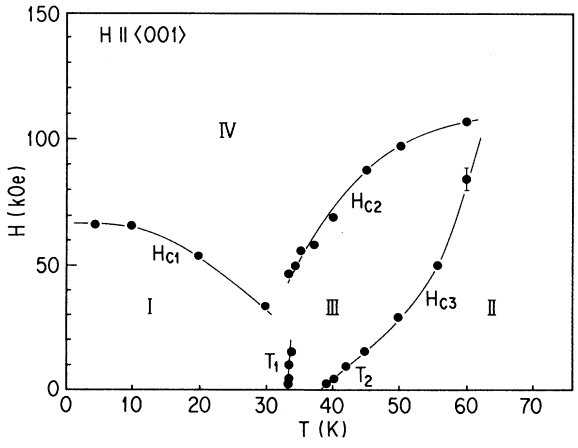

FIG. 3. Magnetic phase diagram of $DyMn_2Ge_2$. The critical fields were determined by the magnetization measurements along the ⟨001⟩ direction. The Néel temperature T_N is 431 K.

calculated intensities, and a and b are extinction parameters.

(2) Because of the large neutron-absorption cross section of natural dysprosium, the absorption of neutrons in the crystal cannot be ignored. Then the absorption factor A_{hkl}, which is the ratio of diffracted intensities with absorption to those without absorption, were calculated by Albrecht's method.[7]

The neutron-diffraction pattern measured at 50 K consists of the nuclear reflection satisfying the condition $h+k+l=$even and three magnetic reflections indexed as (201), (203), and (205). The nuclear intensities were calculated for the following atomic parameters:

Dy atoms on the 2(a) site: $0,0,0;\frac{1}{2},\frac{1}{2},\frac{1}{2}$,

Mn atoms on the 4(d) site: $0,\frac{1}{2},\frac{1}{4};\frac{1}{2},0,\frac{1}{4}$,

$0,\frac{1}{2},\frac{3}{4};\frac{1}{2},0,\frac{3}{4}$,

Ge atoms on the 4(e) site: $0,0,z;0,0,\bar{z}$,

$\frac{1}{2},\frac{1}{2},\frac{1}{2}+z;\frac{1}{2},\frac{1}{2},\frac{1}{2}-z$.

When the Mn and Ge atoms occupy both sites of 4(d) and 4(e), the distribution can be expressed with a site occupation parameter e as follows:

$(1-e)$Mn$+e$Ge on 4(d) site ,

$(1-e)$Ge$+e$Mn on 4(e) site .

Thus the free parameters z, e, a, b, and the Debye-Waller temperature factor B were determined by the least-squares method. The scattering lengths used in this method are 16.9, -3.7, and 8.18 (10^{-13} cm) for the Dy, Mn, and Ge atoms, respectively. The observed and calculated intensities and the evaluated parameters are listed in Tables I and II. The probability of a wrong occupancy of the Mn and Ge atoms at 4(d) and 4(e) sites is negligibly small ($e=0.0033$). The observed magnetic reflections at 50 K resemble those of the high-temperature phase of $R\mathrm{Mn_2Ge_2}$ ($R=$Y, Tb, Er, and Th) (Refs. 8–11) and $R\mathrm{Mn_2Si_2}$ ($R=$Y, Ce, Pr, Nd, Tb, and Er).[9–12] Adopting the magnetic form factor of the Mn^{2+} ion for the Mn atoms, we have analyzed the observed magnetic reflections by assuming a collinear magnetic order with the Mn moments ferromagnetically coupled on the (001) layers and with antiferromagnetic coupling between the adjacent (001) Mn layers. The absence of the ($00l$) ($l=$odd) reflections implies that the magnetic moments are parallel to the c axis. The experimental values of the Mn moment are listed in Table II.

There are two marked differences in the neutron-diffraction patterns between 8 and 50 K: (1) Three magnetic reflections, indexed as (201), (203), and (205), vanish at 8 K. (2) Intensities of all ($h0l$) reflections with $h+k+l=$ even except $h=0$ are greater at 8 K than at 50 K. No superlattice reflections are observed.

Therefore, the change of these intensities is due to the magnetic contribution. The analysis of the observed reflections was performed on the assumption of a collinear ferrimagnetic structure. The magnetic form factor

TABLE I. Calculated and observed integrated intensities for $\mathrm{DyMn_2Ge_2}$. I^M_{calc} is the magnetic contribution to the calculated integrated intensity.

	8 K			35 K			50 K	
(h k l)	I_{obs}	I_{calc}	I^M_{calc}	I_{obs}	I_{calc}	I^M_{calc}	I_{obs}	I_{calc}
0 0 2	3587.2	3729.8	(0)	3585.3	3696.7	(0)	3636.9	3750.5
0 0 4	155.0	145.4	(0)	148.1	142.8	(0)	156.6	147.1
0 0 6	746.0	788.0	(0)	717.5	783.2	(0)	734.6	787.9
0 0 8	910.0	1009.0	(0)	913.2	1009.0	(0)	910.3	965.7
0 0 10	1503.8	1593.0	(0)	1529.5	1601.9	(0)	1335.0	1426.0
1 0 1	2643.1	2658.7	(2564.0)	1101.5	1118.0	(1014.3)	134.3	115.4
1 0 3	2860.6	2716.7	(753.5)	2451.0	2284.5	(278.5)	2112.5	2073.5
1 0 5	2408.7	2221.7	(209.5)	2233.0	2092.1	(76.1)	2181.0	1995.9
2 0 0	2226.3	2266.9	(569.9)	1913.1	1952.9	(236.8)	1690.6	1384.0
2 0 2	2813.1	2832.2	(1371.0)	1981.5	2022.7	(488.2)	1612.4	1557.6
2 0 4	312.7	361.2	(276.2)	202.4	196.0	(110.6)		
2 0 6	829.8	863.9	(303.5)	663.0	675.3	(105.7)	566.3	552.8
2 0 8	870.3	853.0	(59.1)	867.0	825.1	(22.8)	773.8	736.9
2 0 10	1391.7	1412.2	(41.9)	1396.0	1406.1	(15.0)	1149.9	1188.4
3 0 1	476.8	533.7	(493.4)	197.7	223.0	(181.9)	50.3	39.5
3 0 3	1431.8	1400.6	(331.9)	1266.5	1209.7	(122.2)	1113.1	1028.0
3 0 5	1664.0	1546.1	(194.4)	1554.7	1442.7	(71.5)	1369.5	1251.8
3 0 7	256.6	282.5	(112.5)	219.2	212.3	(41.4)	158.3	145.0
4 0 0	1096.0	1108.9	(152.2)	998.8	1033.3	(58.6)	813.9	857.4
4 0 2	1177.5	1154.3	(218.8)	1009.1	1035.0	(78.6)	789.0	833.9
4 0 4	128.7	162.8	(108.4)	71.9	97.1	(41.5)	32.9	47.9
2 0 1	0	0		0	0		101.3	98.3
2 0 3	0	0		0	0		48.3	48.6
2 0 5	0	0		0	0		8.0	15.8

TABLE II. Magnetic moments and parameters refined in the analyses of neutron-diffraction data. The computer fitting program minimized the χ value defined by $\chi=[\sum W(I_{obs}-I_{calc})^2/\sum WI_{obs}^2]^{1/2}$, where W is the weighting function determined from the experimental error of each reflection.

	8 K	35 K	50 K
μ_{Dy}/μ_B	10.2±0.2	6.2	
μ_{Mn}/μ_B	2.3±0.1	1.2	2.2±0.1
σ_s (μ_B/f.u.)	5.6±0.4	3.8	
z	0.3848±0.0002	0.3847	0.3847±0.0002
e			0.0033±0.0004
B (Å)	0.115±0.005	0.045	0.405±0.002
χ	0.047	0.050	0.054

$f_{Dy}(K)$ for the Dy^{3+} ion was approximated by Trammell's formula[13]

$$f_{Dy}(K)=\frac{\mathbf{L}\cdot\mathbf{J}\langle g_0-g_2/2\rangle+2\mathbf{S}\cdot\mathbf{J}\langle j_0\rangle}{\mathbf{L}\cdot\mathbf{J}+2\mathbf{S}\cdot\mathbf{J}},$$

where **J** is the total angular momentum, **L** the total orbital momentum, **S** the total spin, and $\langle g_0-g_2/2\rangle$ and $\langle j_0\rangle$ denote the roles of the orbital and spin scatterings of neutrons, respectively. Since the magnetic (001) reflections are not observed, it is concluded that the Dy and Mn moments are parallel to the c axis. The experimental values of the Dy and Mn moments and refined parameters are listed in Table II. This neutron-diffraction analysis estimated the spontaneous magnetization σ_s as $(5.6\pm0.4)\mu_B$/f.u., which is in good agreement with that obtained by the magnetization measurement at 4.2 K.

Figure 4 shows the temperature dependence of integrated intensities of the (101) and (201) reflections. As seen in this figure, the (101) reflection intensity changes stepwise with two rapidly decreasing processes, which indicate the occurrence of two magnetic transitions, and these two transition temperatures are consistent, respectively, with T_{c1} and T_{c2}, which are determined by the magnetization measurements. The (201) reflection of phases I and III is not observed. The magnetic structure

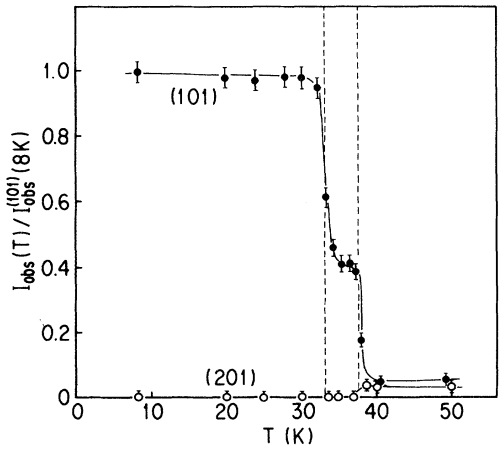

FIG. 4. Temperature dependence of the integrated intensities. The (101) and (201) intensities are indicated by solid and open circles, respectively.

factor of the (101) reflection of phase I is given by $2p_{Dy}$, where p_{Dy} is the magnetic scattering amplitude for the Dy^{3+} ion. Since the (101) intensity hardly depends on temperature below T_{c1}, it is expected that the magnetization of the Dy atom in phase I is maintained constant.

All the reflections observed at 35 K can be analyzed with the same indexes as those at 8 K, and no other magnetic reflections were observed under the present experimental conditions. As shown in Fig. 4, however, the magnetic contribution to the integrated intensity decreases with increasing temperature. Hence we analyzed the reflections observed at 35 K assuming the same magnetic structure as those at 8 K. The values of the Dy and Mn moments and the refinement parameters are listed in Table II. By this neutron-diffraction analysis, the value of σ_s was estimated to be $3.8\mu_B$/f.u., which is small compared with the value obtained by the magnetization measurement.

IV. DISCUSSION

The present neutron-diffraction experiment has revealed that the magnetic structure of phase I is collinear ferrimagnetic, and the Dy and Mn atoms have a magnetic moment of $10\mu_B$ and $2.3\mu_B$, respectively. The value of σ_s evaluated by the neutron-diffraction analysis is consistent with that obtained by the magnetization measurement. Since the value of σ_s and the intensity of the (101) reflection of phase I are almost independent of temperature, the magnetizations of the Dy and Mn atoms are maintained up constant to T_{c1}. Furthermore, it is determined that phase II is a collinear antiferromagnetic structure where the Mn moments on the (001) layer order ferromagnetically and the magnetizations of these layers align antiparallel along the c axis with a $+-+-$ sequence, but the Dy moments remain disordered. This collinear antiferromagnetic structure, however, seems to be inadequate to explain the anisotropic susceptibility observed in $DyMn_2Ge_2$, while this structure is adequate for the case of $GdMn_2Ge_2$,[5] which has the same antiferromagnetic structure in the temperature range from 96.5 to 365 K. As compared with the Gd^{3+} ion ($^8S_{7/2}$) with the electronic configuration of spherical symmetry, the Dy^{3+} ion ($L=5$) has a large single-ion anisotropy, which probably results in the anisotropic susceptibility of $DyMn_2Ge_2$. Since the Mn sublattice is antiferromagnetic in phase II and ferromagnetic in phase I, the Dy-Mn and interlayer Mn-Mn antiferromagnetic exchange interac-

tions in $DyMn_2Ge_2$ compete each other.

The neutron-diffraction pattern of phase III at 35 K is similar to that of phase I, and no magnetic superlattice reflections have been observed for the $(h0l)$ reflections. In this case, the neutron-diffraction pattern has been analyzed by assuming a collinear ferrimagnetic structure. However, this structure and the magnetic moments estimated for the Dy and Mn atoms are inadequate to explain the value of σ_s obtained by the magnetization measurement and the linear field dependence of magnetization. According to the ^{161}Dy Mössbauer study of $DyMn_2Ge_2$,[14] there are two kinds of Dy atoms with different magnetic hyperfine fields in phase III, in spite of the crystallographically equivalent Dy sites. Consequently, these Dy atoms are divided magnetically into two different groups. It should be noted that the Mössbauer effect offers the hyperfine fields of individual Dy nuclei, while neutron diffraction gives the averaged structure through the coherent length of the neutron wave which covers about a thousand lattice points, and that the time needed to observe the elementary process is 3 orders longer for the Mössbauer effect than for neutron diffraction. Therefore, the inconsistency between these experimental results possibly comes from the difference of the observing areas or times. If the magnetic structure of phase III is fluctuating in a very small region compared with the coherent length of neutrons, then it is possible that the averaged magnetic moment obtained by neutron diffraction is small compared with the result of the magnetization measurement. This fluctuation could occur between the two states observed in the Mössbauer measurement.[14] Since a similar phase has never been observed with $GdMn_2Ge_2$,[4,5] phase III of $DyMn_2Ge_2$ could be a consequence of the single-ion anisotropy of the Dy^{3+} ion together with the competition between the Dy-Mn and interlayer Mn-Mn antiferromagnetic exchange interactions.

Since the magnetic field necessary for inducing phase IV is very high, this phase has never been observed by other experimental methods. The value of the magnetization of this phase was estimated to be $7.6\mu_B$/f.u. by extrapolating the magnetization curve above H_{c1} to $H=0$ at 4.2 K and hardly depends on temperature. Since the uniaxial anisotropy of the Dy^{3+} ion is very large and the Dy atom in phase I has the full moment of the Dy^{3+} free ion, it is considered that the transition from phase I to IV is caused by a rearrangement of the Mn moments. From the value of the magnetization, it is considered that phase IV has a canted ferrimagnetic structure; that is, the Dy moments lie along the c axis, while the Mn moments couple ferromagnetically in the (001) layer, but are canted away from the c axis and aligned in opposite directions between adjacent (001) Mn layers as shown schematically in Fig. 5. This structure is stabilized in high magnetic fields due to the competition among the Dy-Mn and Mn-Mn antiferromagnetic exchange interactions and the anisotropy energy of the Mn moments.

V. SUMMARY AND CONCLUSION

The magnetic phase diagram of $DyMn_2Ge_2$ has been determined by the measurement of high-field magnetization. The magnetic structures of four magnetically ordered phases are schematically shown in Fig. 5.

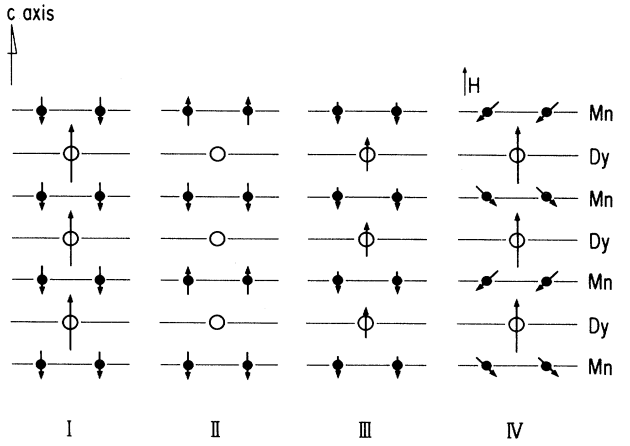

FIG. 5. Schematic magnetic structure of each phase of $DyMn_2Ge_2$. The magnetic structures of phases I and II are determined by neutron diffraction, and that of phase IV is deduced from the magnetization measurement. The magnetic structure in phase III is not uniquely determined, but the average moments at the Dy and Mn atoms are evaluated to be about $6\mu_B$ and $1\mu_B$, respectively.

The magnetic structures of phases I and II have been determined by neutron-diffraction studies. Phase I is a collinear ferrimagnetic structure where the Dy and Mn moments lie along the c axis. The values of the Dy and Mn moments of this phase are $10.2\mu_B$ and $2.3\mu_B$, respectively, and their sublattice magnetizations are maintained constant. Phase II is a collinear antiferromagnetic structure with the Mn moments on (001) layers ferromagnetically coupled with each other and with antiferromagnetic coupling between the adjacent (001) Mn layers, but the Dy moments remain disordered. The Mn moment in phase II is $2.2\mu_B$ at 50 K. These magnetic phases have also been observed with $GdMn_2Ge_2$ and $TbMn_2Ge_2$.[4,5]

The present study shows the first evidence for the existence of phases III and IV. Phase III is probably a consequence of the single-ion anisotropy of the Dy^{3+} ion together with the competition between the Dy-Mn and interlayer Mn-Mn antiferromagnetic exchange interactions. In phase III, the magnetization almost linearly increases with increasing magnetic field. The magnetic structure of phase IV deduced from the magnetization measurements is the canted ferrimagnetic structure where the Dy moments lie along the c axis and the Mn moments are canted away from the c axis and their c plane components make an antiferromagnetic arrangement similar to that of phase II. The magnetization of this phase hardly depends on temperature and magnetic field.

ACKNOWLEDGMENTS

The authors would like to thank Dr. M. Ohashi for the preparation of the $DyMn_2Ge_2$ samples and Dr. H. Kato for his collaboration in the high-field magnetization measurement. The authors also wish to acknowledge valuable discussions with Professor M. Yamada.

[1]H. Pinto, M. Melamud, M. Kuznietz, and H. Shaked, Phys. Rev. B **31**, 508 (1985).
[2]K. S. V. L. Narashimhan, V. U. S. Rao, R. L. Bergner, and W. E. Wallace, J. Appl. Phys. **46**, 4975 (1975).
[3]A. Szytula and I. Szott, Solid State Commun. **40**, 199 (1981).
[4]T. Shigeoka, H. Fujii, H. Fujiwara, K. Yagasaki, and T. Okamoto, J. Magn. Magn. Mater. **31-34**, 209 (1983).
[5]H. Kobayashi, H. Onodera, and H. Yamamoto, J. Magn. Magn. Mater. **79**, 76 (1989).
[6]W. H. Zachariasen, Acta Crystallogr. **23**, 558 (1967).
[7]G. Albrecht, Rev. Sci. Instrum. **10**, 221 (1939).
[8]J. Leciejewicz and A. Szytula, Solid State Commun. **49**, 361 (1984).
[9]Z. Ban, J. Omejec, A. Szytula, and Z. Tomkowicz, Phys. Status Solidi A **27**, 333 (1975).
[10]S. Siek, A. Szytula, and J. Leciejewicz, Solid State Commun. **39**, 863 (1981).
[11]J. Leciejewicz, S. Siek, and A. Szytula, J. Magn. Magn. Mater. **40**, 265 (1984).
[12]T. Shigeoka, N. Iwata, H. Fujii, and T. Okamoto, J. Magn. Magn. Mater. **54-57**, 1343 (1986).
[13]G. T. Trammell, Phys. Rev. **92**, 1387 (1953).
[14]H. Kobayashi, H. Onodera, and H. Yamamoto (unpublished).